PONTIFICIA UNIVERSIDAD CATÓLICA DEL ECUADOR

FACULTAD DE CIENCIAS EXACTAS Y NATURALES

ESCUELA DE CIENCIAS BIOLÓGICAS

F-actin changes and Hippo pathway regulation: An analysis of F-actin in different tumor models of liver cancer

Disertación previa a la obtención del título de Licenciado en Ciencias Biológicas

JOSUÉ PINTO GUALPA

Quito, 2019

A mi familia y amigos, por su apoyo incondicional. Especialmente a mi madre Luz Vicenta Gualpa Jaramillo por ser mi pilar fundamental.

F-actin changes and Hippo pathway regulation: An analysis of F-actin in different tumor models of liver cancer

Josué Pinto Gualpa[1,2], Ruçhan Karaman[2], Oscar D. Perez[1], Alaide Domínguez Calderón[2,3], Georg Halder[2,3]

[1] Escuela de Ciencias Biológicas, Laboratorio de Biología del Desarrollo 113, Pontificia Universidad Católica del Ecuador, Quito, Ecuador

[2] VIB-KU Leuven Center for Cancer Biology, Department of Oncology, KU Leuven, Leuven, Belgium.

[3] Corresponding authors:

alaide.dominguezcalderon@kuleuven.vib.be

mail to: georg.halder@vib.be

KEY WORDS

F-actin; liver cancer; ICC; HCC; Hippo signaling.

ABSTRACT

F-actin is important for multiple cellular processes such as cell adhesion, motility and division. Additionally, it has been demonstrated to play an important role in cancer progression and the regulation of different signaling pathways. Previous studies by our group and others have revealed that, in Drosophila, F-actin acts as an upstream regulator of YAP, the transcriptional effector of the Hippo pathway. However, it remains unknown if actin polymerization is important for YAP activation in mammalian tumors. In this study, we analyzed F-actin levels in cancer cells of four models of liver cancer driven by different oncogenes delivered by hydrodynamic tail vein injection in mice. To compare the levels and localization of F-actin in normal and cancer cells, we used an immunofluorescence assay. We found a striking increase in the levels of F-actin in cancer cells of tumors from intrahepatic cholangiocarcinoma (ICC), hepatocellular carcinoma (HCC) and a combined model of ICC and HCC. Furthermore, the correlation between actin levels and YAP phosphorylation status in tumor cells was analyzed. Immunoblot analysis showed that YAP phosphorylation is significantly decreased in cancer cells of ICC tumors, but only somewhat decreased in cancer cells of HCC tumors. Altogether, our analysis revealed an important correlation in the regulation between the levels of F-actin and the activation status of the Hippo pathway and suggests an essential role of actin polymerization in tumor progression.

INTRODUCTION

Primary liver cancers represent the second most common cause of cancer-related deaths worldwide (Torre *et al.*, 2015). Among primary liver cancers, the most important are intrahepatic cholangiocarcinoma (ICC), combined hepatocellular carcinoma and intrahepatic cholangiocarcinoma (HCC-ICC) and hepatocellular carcinoma (HCC), the latter one being the most prevalent (Maxwell Parkin *et al.*, 2001; Torre *et al.*, 2015; Buettner *et al.*, 2017; Moeini *et al.*, 2017). Current therapies, such as surgical resection or liver transplantation, do not usually succeed due to late diagnosis, high tumor heterogeneity or both (Maxwell Parkin *et al.*, 2001; Zender *et al.*, 2006; Bellentani, 2017). Risk factors which can contribute to liver cancer development include alcohol abuse, toxins, diabetes, obesity, hepatitis B and C (Zender *et al.*, 2006). However, this disease can also be triggered by mutations in key signaling pathways such as the deregulation of the Hippo pathway (Moya and Halder, 2018). Therefore, understanding the signaling pathways underlying the distinct molecular signatures driving genetically different tumor cell subpopulations and liver tumor heterogeneity is essential for the development of effective therapies against all types of liver cancer.

The highly conserved Hippo signaling pathway is emerging as a regulator of organ and tumor growth (Johnson and Halder, 2010; Yimlamai, Fowl and Camargo, 2015) and; therefore, there is a growing interest in understanding the molecular regulation mechanisms of the Hippo pathway and identifying targetable upstream modulators of its activity. The Hippo pathway acts through its downstream effectors Yes-associated-protein (YAP) and WW Domain Containing Transcription Regulator 1 (TAZ) (Wu *et al.*, 2003; Hao *et al.*, 2008). The Hippo signaling axis is composed by Mammalian STE20-like protein kinases 1 & 2 (MST 1/2), which interact with the scaffold protein Salvador Family WW Domain Containing Protein 1 (SAV1) to activate the Large Tumor Suppressor kinases 1 & 2 (LATS 1/2) and their cofactor Monopolar Spindle 1 One Binder (MOB1 A/B) (Harvey, Pfleger and Hariharan, 2003; Hao *et al.*, 2008). Upon activation, LATS 1/2 phosphorylate YAP/TAZ, thus preventing their translocation to the nucleus, resulting in cytoplasmic accumulation via the 14-3-3 complex and posterior degradation by ubiquitin-mediated proteolysis (Vassilev *et al.*, 2001; Basu *et al.*, 2003; Hao *et al.*, 2008; Zhang, Smolen and Haber, 2008; Zhou *et al.*, 2009). On the other hand, upon Hippo pathway inactivation YAP/TAZ remain unphosphorylated and can enter to the nucleus, where they bind to the TEA domain family member 1 (TEAD1) transcriptions factors and

trigger the expression of genes that regulate cell proliferation, stemness and survival (Hao *et al.*, 2008; Zhang *et al.*, 2008; Moya and Halder, 2018). Consequently, YAP/TAZ hyperactivation can trigger the expansion of progenitor cell populations, tissue overgrowth, and eventually lead to cancer initiation in HCC-ICC, ICC and HCC (Zender *et al.*, 2006; Zhou *et al.*, 2009; Lu *et al.*, 2010; Van Haele *et al.*, 2019). Therefore, the downregulation of the MST 1/2 kinases, which prevents YAP/TAZ phosphorylation, induces murine HCC (Lu *et al.*, 2010). Furthermore, combined deletion of SAV1 and MST 1/2 kinases leads to liver overgrowth and HCC in mice (Zhou *et al.*, 2009). In line with this, attenuated expression of LATS 1/2 leads to YAP/TAZ nuclear localization in HCC-ICC mouse model (Zhang *et al.*, 2018) and YAP/TAZ inactivation resulted in the loss of proliferation and tumor growth in ICC (Sugiura *et al.*, 2019). However, little is known about YAP/TAZ interaction with upstream signals during liver cancer and its role in liver tumorigenesis.

Several upstream inputs to the Hippo pathway such as G-protein coupled receptors (GPCRs) and Ras-mitogen-activated protein kinase (MAPK) signaling, as well as actin polymerization and cytoskeleton factors have been identified thus far (Johnson and Halder, 2010; Sansores-Garcia *et al.*, 2011; Aragona *et al.*, 2013; Karaman and Halder, 2018). Specifically, studies have shown that YAP/TAZ activity requires cytoskeletal tension and structural changes of F-actin (Dupont *et al.*, 2011; Sansores-Garcia *et al.*, 2011; Gaspar and Tapon, 2014) and; therefore, F-actin polymerization interruption by capping proteins causes cytoplasmic retention of YAP/TAZ by Hippo-kinase activation in mouse fibroblasts (Densham *et al.*, 2009). Similarly, YAP/TAZ are mechanically regulated by F-actin depolymerization and severing proteins (Fernandez *et al.*, 2011; Aragona *et al.*, 2013). Moreover, upregulation of F-actin polymerization through the silencing of capping proteins causes Hippo downregulation, cell proliferation and tissue overgrowth (Fernandez *et al.*, 2011; Sansores-Garcia *et al.*, 2011; Pocaterra *et al.*, 2019). Despite this evidence, the role of actin and its interaction with the Hippo pathway in primary liver cancers (HCC, ICC and HCC-ICC) remains poorly characterized.

Regulation of F-actin polymerization by overexpression of actin-binding proteins (ABPs) such as tropomyosin 1 (TPM1) cause a reduction in apoptosis and necrosis *in vitro* (Rao and Li, 2004; Schatten, 2015). Upregulation of cofilin, a F-actin depolymerization factor, has been linked to cancer progression and metastasis in breast cancer (Wang, Eddy and Condeelis, 2007; Jiang *et al.*, 2008; Lorente, Syriani and Morales, 2014), prostate cancer (Collazo *et al.*, 2014) and gastric cancer (Wang *et al.*,

2017). Additionally, downstream effectors of Rho GTPases, key regulators of actin dynamics, increase actin polymerization, cell growth, proliferation and survival (Rao and Li, 2004; Izdebska *et al.*, 2018). It has been demonstrated that several amounts of actin are present in cancer cells, but little is known about F-actin role in tumorigenesis (Yamazaki, Kurisu and Takenawa, 2005).

The aim of this study was, therefore, to analyze F-actin expression in liver cancer progression and to investigate a possible regulation of the Hippo pathway trough F-actin. For this purpose, we employed different constructs to induce liver cancer through the activation of: 1) NICD and AKT, to induce ICC (Fan *et al.*, 2012; Chen and Calvisi, 2014), 2) activated mutation of KRasG12V and AKT, for a combined model of HCC-ICC (Ho *et al.*, 2012; Chen and Calvisi, 2014) and 3) c-Myc and activated mutation of NRasG12V (Finisguerra *et al.*, 2015) and 4) activated mutations of KRasG12V and β-cateninS45Y to trigger HCC (Chen and Calvisi, 2014; Tao *et al.*, 2017). We report that, in all tumor models of liver cancer analyzed, F-actin is increased, and p-YAP levels had a tendency to decrease. Our data suggest that F-actin may be important during tumor formation and could act by regulating the Hippo-mediated YAP phosphorylation.

MATERIALS AND METHODS

Constructs and Reagents

The constructs for hydrodynamic injection were pSBbiPuro-HA-myr-AKT, pSBbiPuro-NICD, pSBbiPuro-KRas^{G12V}, pSBbiPuro-β-catenin^{S45Y} and pCaMIN-Myc-NRas^{G12V} alongside the sleeping beauty transposase 11 (SB11). These plasmids were used to transform DH5α competent cells (Invitrogen, Aalst, BE). Plasmids were purified using NucleoSpin Plasmid EasyPure (Macherey-Nagel, Eupen, BE).

Animals

Male wild-type C57BL/6J mice were obtained from The Jackson Laboratory (Bar Harbor, ME USA). All animal experiments were conducted with 6- to 8-week-old mice. Mice were housed, fed, and monitored in accordance with protocols approved by KU Leuven Animal Ethics Committee (Leuven, BE).

Hydrodynamic tail vein injection

The hydrodynamic tail vein injection was performed as previously described (Kim and Ahituv, 2013; Chen and Calvisi, 2014). Briefly, each plasmid and 1 μg of SB 11 transposase were diluted in 0.9% NaCl sterile solution equivalent to 10% of the mouse body weight and injected into the lateral tail vein. The concentrations of the plasmids used are listed in Table 1. For all models, the injection was performed in 5 to 9 sec, and control animals were injected with pSBbiPuro empty plasmid. All animals were carefully monitored for signs of morbidity or discomfort and special attention was paid to the abdominal girth. Animals were euthanized at specific time points (6- to 8-weeks, Table 1) according to the specific tumor model. Livers were dissected and tumoral tissue was snap-frozen in liquid nitrogen and stored at -80°C for further processing and protein extraction.

Immunohistochemistry

Liver specimens were fixed in 4% paraformaldehyde for 2 days, embedded in 4% agarose and cut in 100 μm-thick sections using a Vibratome (Leica VT1000 S). The sections were incubated in 3% bovine serum albumin in PBS, washed 3 times with PBS and incubated overnight at 4°C with the appropriate primary antibodies (listed in Table 2). After rinsing with IF-wash buffer (PBS, 0.1% Tween 20), the sections were incubated with the fluorophore-conjugated secondary antibody (1:500) and DAPI (1:1000) for 2 h at room temperature. Images were acquired using an inverted confocal microscope (Olympus IX83) and processed with the ImageJ software.

Protein extraction and Western Blotting

Frozen mouse liver specimens were lyzed in radio-immuno-precipitation assay (RIPA) buffer (50 mM Tris HCl [pH 8], 150 mM sodium chloride, 1% NP-40, 0.5% sodium deoxycholate, 0.1% SDS) containing the Complete Protease and Phosphatase Inhibitor Cocktail (Roche Molecular Biochemicals). Protein concentrations were determined using the Pierce™ BCA Protein Assay Kit (Thermo Fisher Scientific, Merelbeke, Belgium). Lysated aliquots of 250 μl were denatured by boiling them in 1X Laemmli sample buffer (Bio-Rad, Hercules, CA) containing 5% β-mercaptoethanol, resolved in Mini-PROTEAN TGX Precast Gels (Bio-Rad, Hercules, CA), and transferred to PVDF membranes (ApliChem, Darmstadt, GE). Membranes were blocked in 5%

nonfat dry-milk (Bio-Rad, Hercules, CA) in Tris-buffered saline solution containing 0.1% Tween-20 (TBS-T) for 90 min. Subsequently, the membranes were incubated overnight with the appropriate primary antibodies (listed in Table 3), followed by 3 x 10 min rinses in TBS-T, and on hour incubation with the corresponding horse-radish peroxidase conjugated secondary antibody (Table 3). After rinsing 3 times for 15 min with TBS-T, membranes were developed with GE Healthcare Amersham ECL Prime Western Blotting Detection Reagent (Fisher Scientific, Loughborough, UK).

Statistical Analysis

Data analyses were performed using the GraphPad Prism software 8.0. Data are expressed as means of ± SEM. More detailed information is provided in the corresponding figure caption.

RESULTS

High levels of F-actin correlate with increased YAP activation in ICC tumor cells in mice

To induce ICC in mouse liver, we delivered plasmids by hydrodynamic tail vein injection and overexpressed the intracellular domain of NOTCH1 receptor (NICD), the activated form of human AKT1 (HA-myr-AK1) and the transposase SB11 (Figure 1A). As previously described by Fan *et al.*, (2012), tumors developed within six weeks after injection and, at this time point, animals were euthanized to perform the analyses. NICD-AKT over-expressing livers presented cyst-like cholangiocellular lesions resembling human biliary cyst-adenomas (Figure 1B). The liver/body weight ratio (%) was significantly increased ($p<0.01$) in NICD-AKT livers compared to those of wild-type mice (Figure 1D). To confirm that ICC derived from cells transfected with the NICD-AKT plasmids we immunostained for human influenza hemagglutinin (HA) in tagged tumor cells (Figure 1C). To examine F-actin expression levels and localization in cancer cells, we stained with Alexa Fluor 555 flurophore-conjugated phalloidin, which detects filamentous F-actin. We observed that cancer cells from NICD-AKT tumors showed increased F-actin levels compared to normal liver (Figure 1C), suggesting that cancer cells experience increased levels of mechanical stress. Next, we performed an immunoblotting assay to detect the HA-tag in order to confirm the purity of our samples derived from tumoral tissue and analyzed the levels of actin in cancer vs. normal cells.

Similar to what was observed by immunofluorescence, we found that β-actin levels were increased in tumor samples (Figure 1E). Finally, we attempted to correlate the cellular F-actin levels and to YAP activation. For this purpose, we analyzed YAP phosphorylation by Western Blot. Notably, although we could not detect changes in total YAP protein levels, we observed a marked decrease in YAP phosphorylation in samples from tumor cells in comparison to normal tissue (Figure 1E).

F-actin levels are upregulated in the combined liver cancer model of HCC and ICC in mice

Next, we examined whether the levels of F-actin and pYAP were also elevated in other types of liver tumors. For this purpose, we induced HCC-ICC tumor formation, a highly aggressive liver tumor type that presents combined characteristics of cholangiocarcinoma and hepatocellular carcinoma. We stably overexpressed active forms of KRas (KRas-G12V) and AKT1 (HA-myr-AKT1) with the transposase SB11 in the mouse liver via hydrodynamic tail vein injection (Figure 2A). As described by Ho *et al.*, (2012) the co-expression of myr-AKT1 and $KRas^{G12V}$ in mouse livers generated tumors within 6 weeks and at this time point mice were euthanized, and further analyses were performed (Figure 2B). Ras-AKT livers showed a change in the color, becoming paler, with white areas corresponding to tumor lesions (Figure 2B). To quantify the differences in liver size between wild type and Ras-AKT livers, we measured the liver/body weight ratio (%) and observed a significant increase in Ras-AKT ($p<0,0001$) compared to those of wild type animals (Figure 2D). To trace tumors, we immunostained for the HA tag to verify that HCC-ICC tumors originated from cells overexpressing the Ras-AKT plasmids (Figure 1C). To examine the role of F-actin, we performed phalloidin staining and found that, similarly to the previously described ICC model, cancer cells of this combined HCC-ICC model also presented an increase of F-actin levels in tumor tissue compared to that of normal peritumoral tissue in the liver (Figure 2C). To corroborate the immunostaining data, we performed immunoblotting for HA-tag to confirm that samples are from tumoral tissue, and β-actin to verify the upregulation of F-actin in tumoral tissue (Figure 2E). Furthermore, we analyzed YAP and its phosphorylated state by immunoblotting to reveal a possible interaction between actin and the Hippo pathway. This analysis showed no variation in total YAP levels between tumor and wild-type samples but revealed a slight decrease, albeit non-significant, in YAP phosphorylation in tumor samples (Figure 2E).

Thus, our analyses revealed that cancer cells of the HCC-ICC model also present high levels of F-actin and activated YAP.

Tumor progression in HCC mouse liver cancer models requires F-actin upregulation

To elucidate the relation between F-actin and HCC progression, we used two liver cancer models for HCC: 1) We overexpressed active β-catenin (HA-β-catenin-S45Y) and mutant KRas (KRas-G12V) (Figure 3A), 2). We transfected the Myc oncogene with active NRas (NRas- G12V) (Figure 4A). Noticeable differences in morphology of β-catenin-Ras and Myc-Ras livers were observed in comparison to those of wild-type mice. Based on previous studies performed by Chen and Calvisi, (2014) and Finisguerra *et al.* (2015), β-catenin-Ras and Myc-Ras injections generated tumors within 8 and 6 weeks respectively. At these time points, mice were euthanized to perform the analyses (Figure 3B & 4B). Both, β-catenin-Ras and Myc-Ras livers exhibited substantial number of white spots corresponding to tumors nodules (Figure 3B & 4B) and the β-catenin-Ras livers showed necrosis (Figure 3B, marked with an arrowhead). To verify tissue overgrowth we measured the liver/body weight ratio and observed a dramatic increase in both β-catenin-Ras and Myc-Ras livers ($p<0,001$ and $p<0,0001$ respectively) when compared to that of normal livers (Figure 3D & 4D).

For β-catenin-Ras livers, all tumors were derived from cells that stably overexpressed the HA-β-catenin plasmid (Figure 3C). Due to the lack of a tag in the constructs, e.g. HA, we could not demonstrate that tumors of the Myc-Ras model, derived from the ectopic expression of Myc-Ras plasmid (Figure 4C). To evaluate the role of F-actin in these two models of HCC, we performed a phalloidin staining and observed a significant upregulation of F-actin in tumors in the tissue compared to normal liver (Figure 3C & 4C). Additionally, we performed immunoblotting for HA-tag in β-catenin-Ras samples to confirm that the lysates were from the tumor tissue, and β-actin in both models to corroborate the increase of actin observed by immunohistochemistry (Figure 3E & 4E). Likewise, to show the interaction between actin and the Hippo pathway we analyzed YAP and its phosphorylation at Ser127 by immunoblotting. No changes in total YAP levels were observed in tumor and wild-type samples although we did notice a slight, albeit non-significant, decrease in YAP phosphorylation in tumor samples (Figure 3E & 4E).

DISCUSSION

Characterizing the role of F-actin dynamics during liver tumorigenesis and in controlling different signaling pathways, is fundamental for the development of novel cancer treatments. The role of F-actin has been studied because it has been linked to many types of cancer (Rao and Li, 2004; Dupont *et al.*, 2011; Aragona *et al.*, 2013; Izdebska *et al.*, 2018). Using immunofluorescence and Western-blot assays, we demonstrated that F-actin may play an important role during liver tumorigenesis in different mouse models of liver cancer. More specifically, our results demonstrate that F-actin is upregulated in ICC, HCC-ICC and HCC tumors in the liver. F-actin upregulation was consistent in all the models suggesting that its activity is crucial for tumor formation and progression in the liver. Our results further corroborate previous findings showing actin dynamics is involved in progression of breast, prostate and stomach cancers (Wang, Eddy and Condeelis, 2007; Jiang *et al.*, 2008; Collazo *et al.*, 2014; Lorente, Syriani and Morales, 2014; Wang *et al.*, 2017). Furthermore, our results show that actin dynamics could also plays a role during liver cancer development. However, our data do not allow to determine whether F-actin controls tumor progression or tumor development, so further studies examining F-actin during tumor initiation are required.

F-actin is important for many cellular processes, such as cell polarity, adhesion, motility and division (Stevenson, Veltman and Machesky, 2012) and; therefore, changes in its dynamics can affect the activity of many different signaling pathways (Stevenson, Veltman and Machesky, 2012; Schatten, 2015). Our data reveal that YAP phosphorylation levels tend to decrease, albeit non-significative, in ICC-HCC and HCC tumors but are reduced in ICC tumors, suggesting that actin upregulation could decrease the phosphorylated form of YAP during liver tumorigenesis. These results are consistent with previous studies which suggest that F-actin regulates the Hippo pathway where loss of capping proteins increased cell proliferation and overgrowth by increasing F-actin levels and inactivating the Hippo pathway (Fernandez *et al.*, 2011; Sansores-Garcia *et al.*, 2011). Furthermore, the significant and slight decrease in p-YAP levels in the ICC and the combined HCC-ICC models respectively, could be explained by the transformation of hepatocytes into biliary epithelial cells (BEC's) during tumor formation due to the fact that YAP is required for survival and maintenance of BEC's in the liver (Pepe-Mooney *et al.*, 2019). In line with this, *in vitro* studies showed that decrease of actin polymerization by silencing of Rho GTPases and chemical agents such as Latrunculin A

and Cytochalasin D inhibited YAP transcriptional activity (Dupont *et al.*, 2011; Sansores-Garcia *et al.*, 2011). Consistently, promoting actin polymerization by upregulation of the active diaphanous protein (DIAPH1) stimulates YAP activity (Dupont *et al.*, 2011; Sansores-Garcia *et al.*, 2011). To fully elucidate the role of F-actin during liver tumorigenesis in ICC, combined HCC-ICC and HCC, further investigations regarding formins, Arp2/3, Rho GTPases and capping proteins and other factors involved in actin polymerization are necessary, along with studies aimed to unravel the precise role of F-actin in Hippo pathway inactivation.

ACKNOWLEDGMENTS

This project was funded by grants from the Research Foundation Flanders (FWO) to ADC. We would like to thank Xin Chen, Perry Hackett, Channing Der, Clark Distelhorst, and Eric Kowarz for depositing plasmids at Addgene, and Leen Van Huffel for providing mouse strains. We would also like to thank all members of Halder's Laboratory of Growth Control and Cancer Research at KU Leuven for their help and knowledge and the Laboratory of Developmental Biology at Pontificia Universidad Católica del Ecuador (PUCE) for their support.

REFERENCES

1. Aragona, M. *et al.* (2013) 'A Mechanical Checkpoint Controls Multicellular Growth through YAP/TAZ Regulation by Actin-Processing Factors', *Cell*. Elsevier Inc., 154(5), pp. 1047–1059. doi: 10.1016/j.cell.2013.07.042.
2. Basu, S. *et al.* (2003) 'Akt phosphorylates the Yes-associated protein, YAP, to induce interaction with 14-3-3 and attenuation of p73-mediated apoptosis.', *Molecular cell*, 11(1), pp. 11–23. Available at: http://www.ncbi.nlm.nih.gov/pubmed/12535517.
3. Bellentani, S. (2017) 'The epidemiology of non-alcoholic fatty liver disease', *Liver International*, 37(October 2016), pp. 81–84. doi: 10.1111/liv.13299
4. Buettner, S. *et al.* (2017) 'Intrahepatic cholangiocarcinoma: Current perspectives', *OncoTargets and Therapy*, 10, pp. 1131–1142. doi: 10.2147/OTT.S93629.
5. Chen, X. and Calvisi, D. F. (2014) 'Hydrodynamic transfection for generation of novel mouse models for liver cancer research', *American Journal of Pathology*. American Society for Investigative Pathology, 184(4), pp. 912–923. doi: 10.1016/j.ajpath.2013.12.002.
6. Collazo, J. *et al.* (2014) 'Cofilin drives cell-invasive and metastatic responses to TGF-β in prostate cancer', *Cancer Research*, 74(8), pp. 2362–2373. doi: 10.1158/0008-5472.CAN-13-3058.
7. Densham, R. M. *et al.* (2009) 'MST Kinases Monitor Actin Cytoskeletal Integrity and Signal via c-Jun N-Terminal Kinase Stress-Activated Kinase To Regulate p21Waf1/Cip1 Stability', *Molecular and Cellular Biology*, 29(24), pp. 6380–6390. doi: 10.1128/mcb.00116-09.
8. Dupont, S. *et al.* (2011) 'Role of YAP/TAZ in mechanotransduction', *Nature*, 474(7350), pp. 179–184. doi: 10.1038/nature10137.
9. Fan, B. *et al.* (2012) 'Cholangiocarcinomas can originate from hepatocytes in mice', *Journal of Clinical Investigation*, 122(8), pp. 2911–2915. doi: 10.1172/JCI63212.
10. Fernandez, B. G. *et al.* (2011) 'Actin-Capping Protein and the Hippo pathway regulate F-actin and tissue growth in Drosophila', *Journal of Cell Science*, 124(11), pp. e1–e1. doi: 10.1242/jcs.092866.
11. Finisguerra, V. *et al.* (2015) 'MET is required for the recruitment of anti-tumoural neutrophils', *Nature*, 522(7556), pp. 349–353. doi: 10.1038/nature14407.

12. Gaspar, P. and Tapon, N. (2014) ‘Sensing the local environment: Actin architecture and Hippo signalling’, *Current Opinion in Cell Biology*. Elsevier Ltd, 31, pp. 74–83. doi: 10.1016/j.ceb.2014.09.003.
13. Van Haele, M. *et al.* (2019) ‘YAP and TAZ Heterogeneity in Primary Liver Cancer: An Analysis of Its Prognostic and Diagnostic Role’, *International journal of molecular sciences*, 20(3). doi: 10.3390/ijms20030638.
14. Hao, Y. *et al.* (2008) ‘Tumor suppressor LATS1 is a negative regulator of oncogene YAP’, *Journal of Biological Chemistry*, 283(9), pp. 5496–5509. doi: 10.1074/jbc.M709037200.
15. Harvey, K. F., Pfleger, C. M. and Hariharan, I. K. (2003) ‘The Drosophila Mst Ortholog, hippo, Restricts Growth and Cell Proliferation and Promotes Apoptosis’, *Cell*, 114, pp. 457–467. doi: 10.1016/S0092-8674(03)00557-9.
16. Ho, C. *et al.* (2012) ‘AKT and N-Ras co-activation in the mouse liver promotes rapid carcinogenesis via mTORC1, FOXM1/SKP2, and c-Myc pathways’, *Hepatology*, 55(3), pp. 833–845. doi: 10.1002/hep.24736.AKT.
17. Izdebska, M. *et al.* (2018) ‘The Role of Actin Dynamics and Actin-Binding Proteins Expression in Epithelial-to-Mesenchymal Transition and Its Association with Cancer Progression and Evaluation of Possible Therapeutic Targets’, *BioMed Research International*, 2018, pp. 1–13. doi: 10.1155/2018/4578373.
18. Jiang, P. *et al.* (2008) ‘An actin-binding protein girdin regulates the motility of breast cancer cells’, *Cancer Research*, 68(5), pp. 1310–1318. doi: 10.1158/0008-5472.CAN-07-5111.
19. Johnson, R. L. and Halder, G. (2010) ‘Hippo signaling: growth control and beyond’, *Development*, 138(1), pp. 9–22. doi: 10.1242/dev.045500.
20. Karaman, R. and Halder, G. (2018) ‘Cell junctions in Hippo signaling’, *Cold Spring Harbor Perspectives in Biology*, 10(5). doi: 10.1101/cshperspect.a028753.
21. Kim, M. J. and Ahituv, N. (2013) ‘The Hydrodynamic Tail Vein Assay as a Tool for the Study of Liver Promoters and Enhancers’, *Methods Molecular Biology*, 1015, pp. 279–289. doi: 10.1007/978-1-62703-435-7.
22. Lorente, G., Syriani, E. and Morales, M. (2014) ‘Actin filaments at the leading edge of cancer cells are characterized by a high mobile fraction and turnover regulation by profilin I’, *PLoS ONE*, 9(1). doi: 10.1371/journal.pone.0085817.
23. Lu, L. *et al.* (2010) ‘Hippo signaling is a potent in vivo growth and tumor suppressor pathway in the mammalian liver’, *Proceedings of the National Academy of*

Sciences, 107(4), pp. 1437–1442. doi: 10.1073/pnas.0911427107.

24. Maxwell Parkin, D. *et al.* (2001) 'Estimating the world cancer burden: Globocan 2000', *International Journal of Cancer*, 94(2), pp. 153–156. doi: 10.1002/ijc.1440.

25. Moeini, A. *et al.* (2017) 'Mixed hepatocellular cholangiocarcinoma tumors: Cholangiolocellular carcinoma is a distinct molecular entity', *Journal of Hepatology*. European Association for the Study of the Liver, 66(5), pp. 952–961. doi: 10.1016/j.jhep.2017.01.010.

26. Moya, I. M. and Halder, G. (2018) 'Hippo–YAP/TAZ signalling in organ regeneration and regenerative medicine', *Nature Reviews Molecular Cell Biology*. doi: 10.1038/s41580-018-0086-y.

27. Pepe-Mooney, B. J. *et al.* (2019) 'Single-Cell Analysis of the Liver Epithelium Reveals Dynamic Heterogeneity and an Essential Role for YAP in Homeostasis and Regeneration', *Cell Stem Cell*. Elsevier Inc., 25(1), pp. 23-38.e8. doi: 10.1016/j.stem.2019.04.004.

28. Pocaterra, A. *et al.* (2019) 'F-actin dynamics regulates mammalian organ growth and cell fate maintenance', *Journal of Hepatology*. European Association for the Study of the Liver, 71(1), pp. 130–142. doi: 10.1016/j.jhep.2019.02.022.

29. Rao, J. and Li, N. (2004) 'Microfilament actin remodeling as a potential target for cancer drug development.', *Current cancer drug targets*, 4(4), pp. 345–54. Available at: http://www.ncbi.nlm.nih.gov/pubmed/15180500.

30. Sansores-Garcia, L. *et al.* (2011) 'Modulating F-actin organization induces organ growth by affecting the Hippo pathway', *EMBO Journal*, 30(12), pp. 2325–2335. doi: 10.1038/emboj.2011.157.

31. Schatten, H. (2015) *The cytoskeleton in health and disease*, *The Cytoskeleton in Health and Disease*. doi: 10.1007/978-1-4939-2904-7.

32. Stevenson, R. P., Veltman, D. and Machesky, L. M. (2012) 'Actin-bundling proteins in cancer progression at a glance', *Journal of Cell Science*, 125(5), pp. 1073–1079. doi: 10.1242/jcs.093799.

33. Sugiura, K. *et al.* (2019) 'The Expression of Yes-Associated Protein (YAP) Maintains Putative Cancer Stemness and Is Associated with Poor Prognosis in Intrahepatic Cholangiocarcinoma', *The American Journal of Pathology*. American Society for Investigative Pathology, 189(9), pp. 1863–1877. doi: 10.1016/j.ajpath.2019.05.014.

34. Tao, J. *et al.* (2017) 'Targeting β-catenin in hepatocellular cancers induced by

co-expression of mutant β-catenin and K-Ras in mice', 65(5), pp. 1581–1599. doi: 10.1002/hep.28975.TARGETING.

35. Torre, L. A. *et al.* (2015) 'Global Cancer Statistics, 2012', *CA: A Cancer Journal for Clinicians*, 65(2), pp. 87–108. doi: 10.3322/canjclin.55.2.74.

36. Vassilev, A. *et al.* (2001) 'TEAD/TEF transcription factors utilize the activation domain of YAP65, a Src/Yes-associated protein localized in the cytoplasm', *Genes and Development*, 15(10), pp. 1229–1241. doi: 10.1101/gad.888601.

37. Wang, H. *et al.* (2017) 'Cofilin 1 induces the epithelial-mesenchymal transition of gastric cancer cells by promoting cytoskeletal rearrangement', *Oncotarget*, 8(24), pp. 39131–39142. doi: 10.18632/oncotarget.16608.

38. Wang, W., Eddy, R. and Condeelis, J. (2007) 'The cofilin pathway in breast cancer invasion and metastasis', *Nature Reviews Cancer*, 7(6), pp. 429–440. doi: 10.1038/mp.2011.182.doi.

39. Wu, S. *et al.* (2003) 'hippo encodes a Ste-20 family protein kinase that restricts cell proliferation and promotes apoptosis in conjunction with salvador and warts', *Cell*, 114(4), pp. 445–456. doi: 10.1016/S0092-8674(03)00549-X.

40. Yamazaki, D., Kurisu, S. and Takenawa, T. (2005) 'Regulation of cancer cell motility through actin reorganization', *Cancer Science*, 96(7), pp. 379–386. doi: 10.1111/j.1349-7006.2005.00062.x.

41. Yimlamai, D., Fowl, B. H. and Camargo, F. D. (2015) 'Emerging evidence on the role of the Hippo/YAP pathway in liver physiology and cancer', *Journal of Hepatology*. European Association for the Study of the Liver, 63(6), pp. 1491–1501. doi: 10.1016/j.jhep.2015.07.008.

42. Zender, L. *et al.* (2006) 'Identification and validation of oncogenes in liver cancer Supplemental Data', *Cell*, 125(7), pp. 1253–67. doi: 10.1016/j.cell.2006.05.030.

43. Zhang, J., Smolen, G. A. and Haber, D. A. (2008) 'Negative regulation of YAP by LATS1 underscores evolutionary conservation of the Drosophila Hippo pathway', *Cancer Research*, 68(8), pp. 2789–2794. doi: 10.1158/0008-5472.CAN-07-6205.

44. Zhang, L. *et al.* (2008) 'The TEAD/TEF family of transcription factor Scalloped mediates Hippo signaling in organ size control', *Dev Cell*, 14(3), pp. 377–387. doi: 10.1016/j.devcel.2008.01.006.The.

45. Zhang, S. *et al.* (2018) 'Hippo Cascade Controls Lineage Commitment of Liver Tumors in Mice and Humans', *American Journal of Pathology*. American Society for Investigative Pathology, 188(4), pp. 995–1006. doi: 10.1016/j.ajpath.2017.12.017.

46. Zhou, D. *et al.* (2009) 'Mst1 and Mst2 Maintain Hepatocyte Quiescence and Suppress Hepatocellular Carcinoma Development through Inactivation of the Yap1 Oncogene', *Cancer Cell*. Elsevier Ltd, 16(5), pp. 425–438. doi: 10.1016/j.ccr.2009.09.026.

TABLES

Tumor type	Plasmids	Concentration (μg/ml)	Latency
HCC	pSBbiPuro-KRas^{G12V}	10	~8 weeks
	pSBbiPuro-β-catenin^{S45Y}	10	
HCC	pCaMIN-Myc-NRas^{G12V}	10	~6 weeks
Mixed HCC and ICC	pSBbiPuro-KRas^{G12V}	10	~6 weeks
	pSBbiPuro-HA-myr-AKT	4	
ICC	pSBbiPuro-NICD	20	~6 weeks
	pSBbiPuro-HA-myr-AKT	4	

Table 1 Plasmid concentrations used to induce liver cancer in mice

Antibody	Company	Catalog number	Dilution
OPN	R&D systems (Abingdon, UK)	AF1433	1:300
Phalloidin A-555	Cell signaling Technology (Danvers, MA USA)	13054S	1:50
HA-tag	Sigma-Aldrich (Overijse, BE)	11867423001	1:200
β-catenin	Cell Signaling Technology	8814S	1:200

Table 2 Immunohistochemistry Primary Antibody Information

Antibody	Company	Catalog number	Dilution
β-Actin	Abcam (Cambridge, MA)	Ab8227	1:1000
YAP	Novus Biologicals (Oxon, UK)	NB110-58358	1:2000
HA-tag	Sigma-Aldrich (Overijse, BE)	11867423001	1:1000
p-YAP (S127)	Cell Signaling Technology	4911S	1:1000
GAPDH	Invitrogen	AM4300	1:2000
Goat anti-rabbit HRP	Thermo Fisher Scientific (Merelbeke, Belgium)	A24531	1:5000
Goat anti-rat HRP	Thermo Fisher Scientific	31470	1:5000
Goat anti-mouse HRP	Thermo Fisher Scientific	31432	1:10000

Table 3 Western Blotting Antibody Information

FIGURES

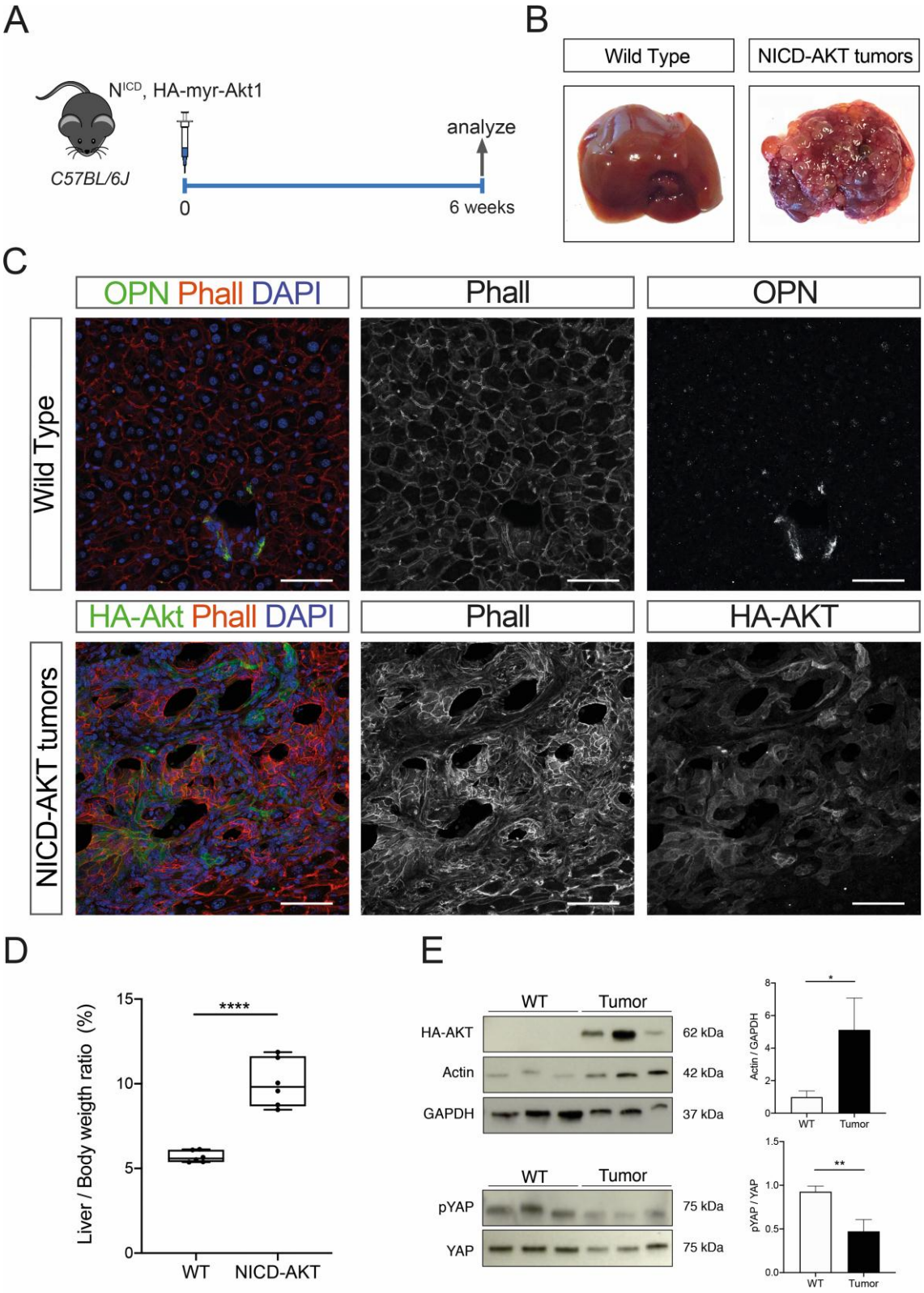

Figure 1. F-actin is upregulated in NICD-AKT tumor model for ICC. (**A**) Scheme showing the performance of hydrodynamic tail vein injection in C57BL/6J mice with the NICD-AKT plasmids. Tumors were analyzed 6 weeks after plasmid injection. (**B**)

Macroscopic images of wild type (left panel) and NICD-AKT (right panel) livers 6 weeks post injection. (**C**) Immunostaining for phalloidin (red), Osteopontin (OPN) in wild type and HA-tag in NICD-AKT (green) and DAPI (blue) in liver. Scale bar is equal to 60 μm. (**D**) Tumor burden effect in NICD-AKT model vs. wild type mice. Values are means ± SEM of 6 animals; **** p=0.0072, unpaired two-tailed *t*-test. (**E**) Representative immunoblotting showing β-actin, YAP and pYAP levels in wild type and NICD-AKT mice. Values are means ± SEM from 3 different mice; * p=0.0231 for actin/GAPDH and ** p=0.0063 for pYAP/YAP, unpaired two tailed *t*-test.

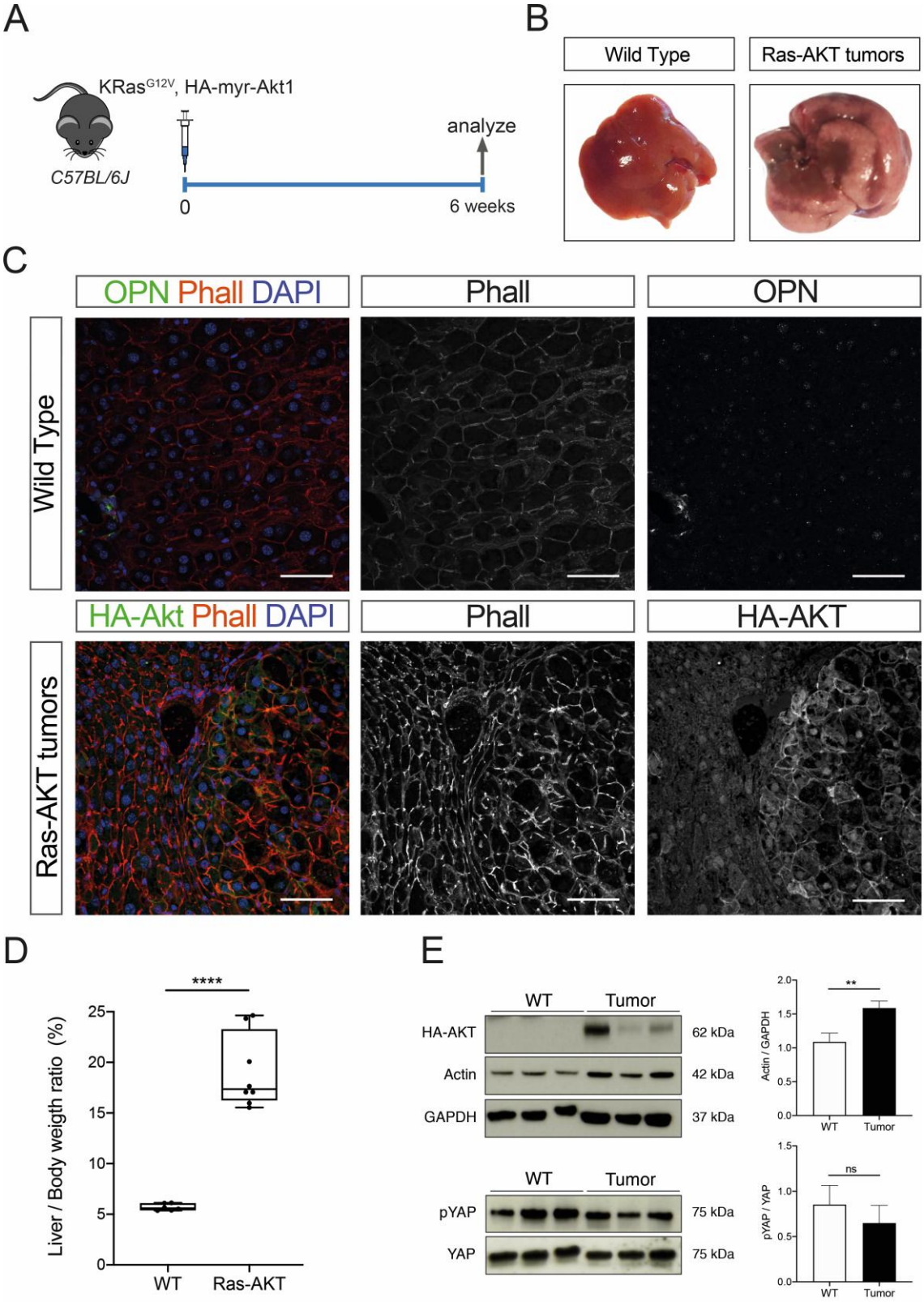

Figure 2. F-actin is upregulated in Ras-AKT liver cancer model for combined HCC-ICC. (**A**) Scheme showing the performance of hydrodynamic tail vein injection in C57BL/6J mice with the Ras-AKT plasmids. Tumors were analyzed 6 weeks after plasmid injection. (**B**) Macroscopic images of wild type (left panel) and Ras-AKT (right panel) livers 6

weeks post injection. (**C**) Immunostaining for phalloidin (red), OPN in wild type and HA-tag in Ras-AKT (green) and DAPI (blue) in liver. Scale bar is equal to 60 μm. (**D**) Effect in tumor burden in Ras-AKT model vs wild type. Values are means ± SEM from 6 to 8 animals; **** $p<0.001$, unpaired two tailed *t*-test. (**E**) Representative immunoblotting showing β-actin, YAP and pYAP levels in wild type and Ras-AKT mice. Values are means ± SEM from 3 different mice; ** $p=0.0064$ for actin/GAPDH and non-significant (ns) for pYAP/YAP, unpaired two tailed *t*-test.

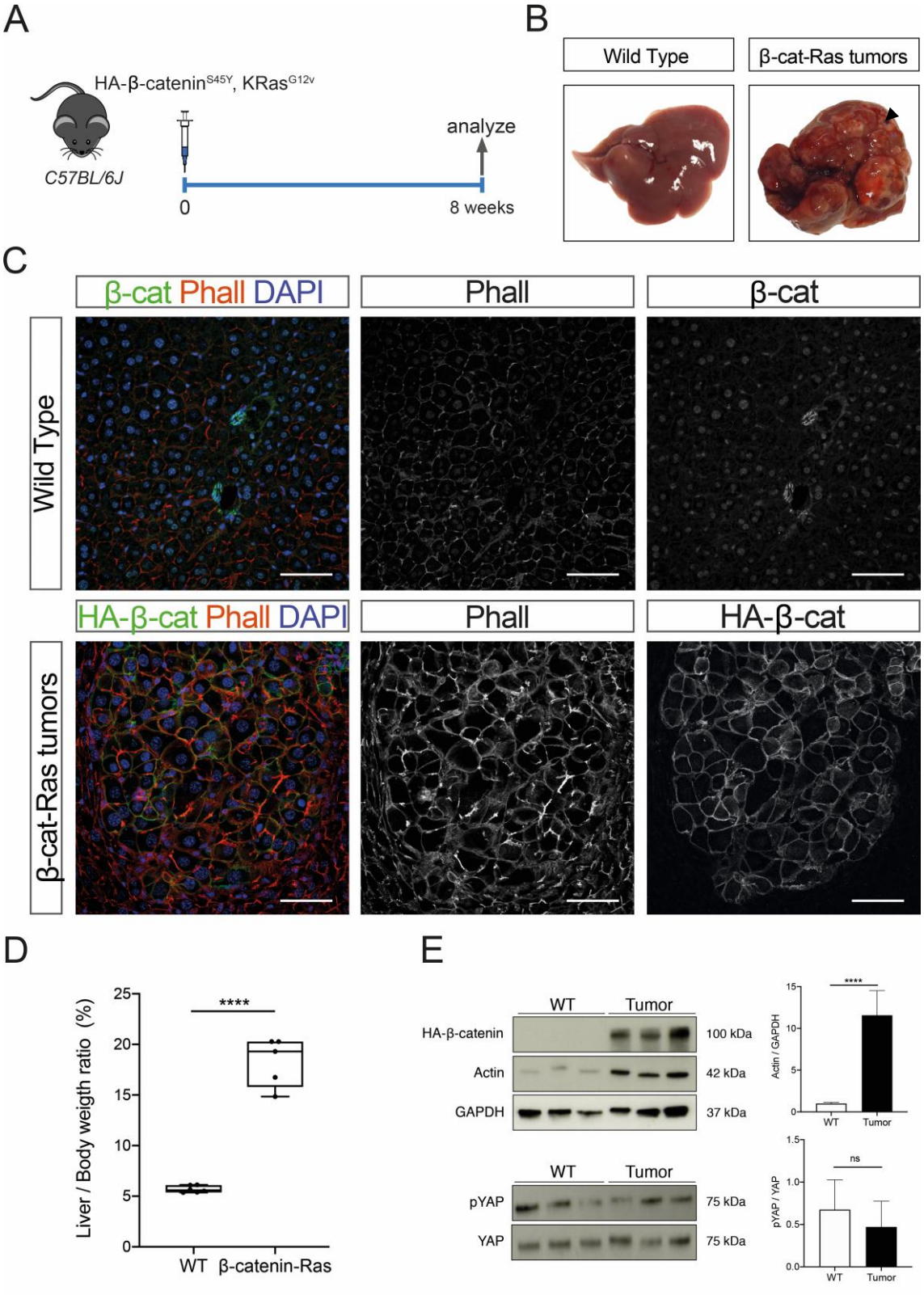

Figure 3. Induction of HCC by β-catenin-Ras shows upregulation in F-actin levels. (**A**) Scheme showing the performance of hydrodynamic tail vein injection in C57BL/6J mice with the β-catenin-Ras plasmids. Tumors were analyzed 8 weeks after plasmid injection. (**B**) Macroscopic images of wild type (left panel) and β-catenin-Ras (right panel) livers 8

weeks post injection. (**C**) Immunostaining for phalloidin (red), β-catenin in wild type and HA-β-catenin in β-catenin-Ras (green) and DAPI (blue) livers slides. Scale bar is equal to 60 μm. (**D**) Effect in tumor burden in β-catenin-Ras model vs wild type. Values are means ± SEM from 5 to 6 animals; **** p=0.0006, unpaired two tailed *t*-test. (**E**) Representative immunoblotting showing β-actin, YAP and pYAP levels in wild type and β-catenin-Ras mice. Values are means ± SEM from 3 different mice; **** p<0.0001 for actin/GAPDH and non-significant (ns) for pYAP/YAP, unpaired 2-tailed Student's *t*-test.

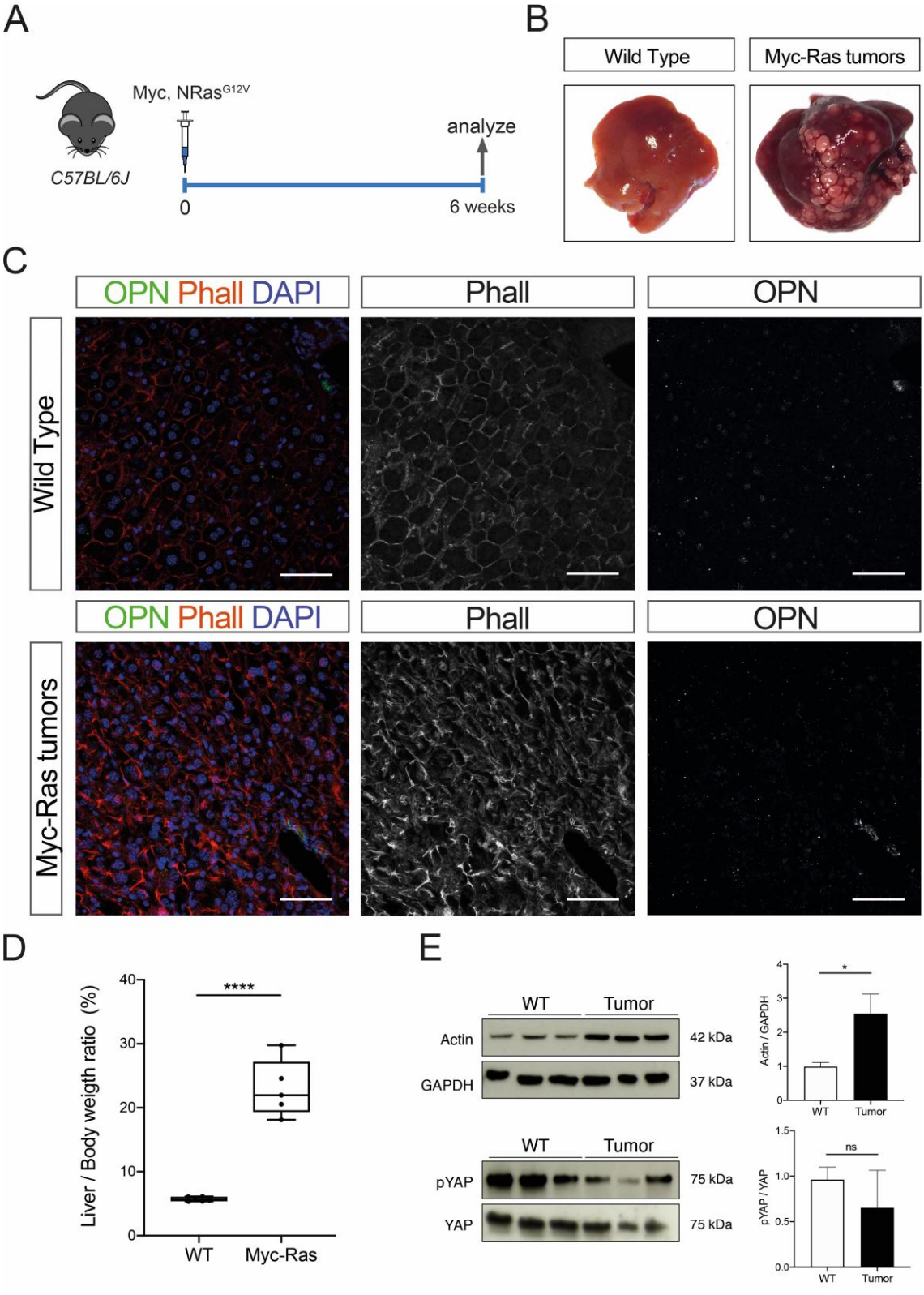

Figure 4. Myc-Ras trigger HCC formation and F-actin upregulation. (**A**) Scheme showing the performance of hydrodynamic tail vein injection in C57BL/6J mice with the Myc-Ras plasmid. Tumors were analyzed 6 weeks post injection. (**B**) Macroscopic images of wild type (left panel) and Myc-Ras (right panel) livers 6 weeks post injection.

(**C**) Immunostaining for phalloidin (red), OPN (green) and DAPI (blue) in wild type and Myc-Ras liver. Scale bar is equal to 60 μm. (**D**) Effect in tumor burden in Myc-Ras model vs wild type. Values are means ± SEM from 5 to 6 animals; **** $p<0.0001$, unpaired two tailed *t*-test. (**E**) Representative immunoblotting showing β-actin, YAP and pYAP levels in wild type and Myc-Ras mice. Values are means ± SEM from 3 different mice; * $p<0.0103$ for actin/GAPDH and non-significant (ns) for pYAP/YAP, unpaired two tailed *t*-test.